Jpn. J. Appl. Phys. Vol. 38 (1999) pp. 1–6
Part 1, No. 1A, January 1999
©1999 Publication Board, Japanese Journal of Applied Physics

Novel Bonding Technology for Hermetically Sealed Silicon Micropackage

Duck-Jung LEE[1,*], Byeong-Kwon JU[1], Woo-Beom CHOI[1], Jee-Won JEONG[1], Yun-Hi LEE[1], Jin JANG[2], Kwang-Bae LEE[3] and Myung-Hwan OH[1]

[1]*Electronic Materials and Devices Research Center, Korea Institute of Science and Technology, P.O. Box 131, Cheongryang, Seoul 130-650, Korea*
[2]*Department of Physics, Kyunghee University, Hoigi-dong, Dongdaemun-gu, Seoul 130-701, Korea*
[3]*Department of Physics, Sangji University, Usan-dong, Wonju 220-702, Korea*

(Received February 13, 1998; accepted for publication September 4, 1998)

We performed glass-to-silicon bonding and fabricated a hermetically sealed silicon wafer using silicon direct bonding followed by anodic bonding (SDAB). The hydrophilized glass and silicon wafers in solution were dried and initially bonded in atmosphere as in the silicon direct bonding (SDB) process, but annealing at high temperature was not performed. Anodic bonding was subsequently carried out for the initially bonded specimens. Then the wafer pairs bonded by the SDAB method were different from those bonded by the anodic bonding process only. The effects of the bonding process on the bonded area and tensile strength were investigated as functions of bonding temperature and voltage. Using scanning electron microscopy (SEM), the cross-sectional view of the bonded interface region was observed. In order to investigate the migration of the sodium ions in the bonding process, the concentration of the bonded glass was compared with that of standard glass. The specimen bonded using the SDAB process had higher efficiency than that using the anodic bonding process only.

KEYWORDS: hydrophilization, anodic bonding, SDAB, tensile strength, SIMS analysis, hermetic sealing

1. Introduction

The bonding process of two wafers is of interest recently for micropackaging of microelectromechanical devices.[1,2] Especially in the case of glass-to-silicon bonding, anodic bonding, which does not require a post heat treatment at high temperature, has become a promising technique. Anodic bonding seems to be a simple process, but it provides a strong, hermetic seal which protects the actuator sensors from the atmosphere.[3,4] Anodic bonding can be applied to achieve the structure required of pressure and acceleration sensors. Since the invention of anodic bonding in 1969 by Wallis and Pomerantz,[5] Pyrex #7740 glass having nearly the same thermal expansion coefficient as silicon, has usually been used for it.[6] Glass-to-silicon anodic bonding has generally been used for making microsensors and microactuators.[7]

Anodic bonding occurs as a consequence of the high level of electric pressure applied during the process. The metal or semiconductor is positive with respect to the glass. A high temperature is necessary to increase the ion mobility. When the dc voltage is applied, the positive ions in the glass, mainly Na^+, move to the negative electrode forming a depletion layer. The depletion layer is formed in the glass close to the metal or semiconductor surface. As a consequence, a high electrostatic field is generated that pulls the surfaces together, allowing the formation of atomic bonds. The bonding process at a high temperature induces a higher thermal residual stress. Built in stress could negatively affect the device's performance. However, lowering the bonding temperature can reduce the mechanical strength in the bonded structure and the thermal residual stress.

In order to obtain the profile of electrostatic force, Poisson's equation must be solved.[8] The equation for the glass is

$$\frac{d^2V}{dx^2} = -\frac{dE}{dx} = -\frac{Q(x)}{\varepsilon_g} = \frac{qN_0}{\varepsilon_g}, \qquad (1)$$

where $Q(x)$ is the charge in the depletion region due to the presence of the fixed negative ions, ε_g is the dielectric constant of the deposited glass layer, q is the electron charge and N_0 is the fixed negative ion concentration in the bulk glass.

From eq. (1), using the boundary condition, the electrostatic force P between the glass and silicon is given by

$$P = \frac{1}{2}\varepsilon_0 E^2 = \frac{1}{2}\varepsilon_0\left(\frac{qN_0x_p}{\varepsilon_0}\right)^2 = \varepsilon_g qN_0V_p, \qquad (2)$$

where x_p is the length of the depletion region and V_p is the potential at $x = x_p$. Therefore, electrostatic force increases as applied voltage increases. Furthermore, the increase of temperature results in a higher diffusion rate of the sodium ions (increase of x_p).

Silicon direct bonding (SDB) is a process in which two separate wafers are brought into contact at room temperature and then annealed in a furnace. When two wafers with highly hydrophillic or hydrophobic surfaces are brought into contact at room temperature, an initial bond is formed via Van der Waals forces at the surface. If subsequently annealed at a high temperature (>700°C) in dry oxygen or an inert ambient, the native oxides of the weakly bonded wafer pair merge to form a contiguous SiO_2 layer that attaches bonds them .[9,10] Direct bonding has commonly been used for bonding silicon-silicon wafers.[11]

In this silicon direct bonding followed by anodic bonding (SDAB) process, the microgap existing between two wafers is reduced by the initial bonding of hydrophilized wafers. The electrostatic force between wafers is higher than in the case of anodic bonding only. Therefore, the SDAB method was newly developed to obtain a wide bonded area and a higher tensile strength, even if the glass wafer possesses a rough surface. The improved bonding properties were discussed in terms of the measured tensile strength, current-time curve and the secondary ion mass spectroscopy (SIMS) analysis before and after the bonding process. The thermal residual stress is generated by the anodic bonding process. The bonding process at a high temperature induces a high thermal residual stress. The thermal stress is an important factor in micromachined mechanical sensors. However, generated stress could negatively affect the device performance. In particular, lower

* E-mail: djlee@kistmail.kist.re.kr

bonding temperature can reduce the mechanical strength in the bonded structure despite the advantage of lower thermal residual stress.

2. Experimental

The anodic bonding process is as follows. A cleaned silicon wafer is held against a cleaned glass wafer, and the glass-to-silicon assembly is placed on a hot plate. A typical experimental setup for anodic bonding is illustrated in Fig. 1. A positive electrode is attached to the silicon wafer, and an additional electrode is attached to the glass wafer. A dc voltage is then applied across the electrodes at the elevated temperature. The electric field builds up across the silicon/glass interface and serves to pull the two wafers into contact.

The materials used in the bonding experiments were n-type silicon wafers which were 200 μm thick, 1–10 $\Omega|\cdot$cm, 1 inch in diameter and (100)-oriented, and Corning #7740 glass wafers which were the 500 μm thick and 1 inch in diameter. The glass-to-silicon bonding was carried out by two procedures and the bonded specimens were therefore classified into two groups. The samples belonging to group A were bonded using only anodic bonding performed at temperatures in the range of 200–300°C with a dc voltage in the range of 60–300 V. The applied voltage was turned off after cooling to prevent back-diffusion of the sodium ions. The samples belonging to group B were initially bonded following to the SDB steps without high-temperature annealing. The initially bonded wafer pairs in group B were left for 24 h at room temperature to allow the H_2O existing between glass and silicon to dry completely. Then, anodic bonding was carried out on the initially bonded specimens.

The bonding process using SDAB can be described as follows.

(Silicon and Pyrex #7740 glass wafers were treated under the same condition.)

1) RCA cleaning
2) (In the case of SDAB) Hydrophilization: dipping in $H_2O/H_2O_2/NH_4OH$ (6 : 1 : 4) solution for 2–3 min at 55–60°C
3) Rinsing with deionized water
4) Spin drying
5) Initial bonding by direct bonding method
6) Anodic bonding for initially bonded specimen

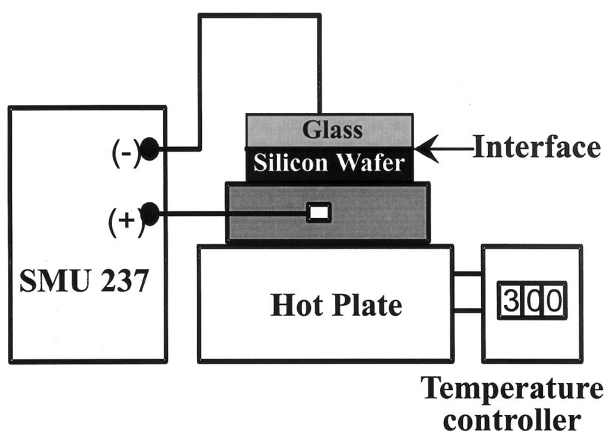

Fig. 1. Experimental setup for anodic bonding.

The surface morphology was investigated through atomic force microscope (AFM) analysis. The tensile strength of bonded specimens was investigated as functions of bonding temperature and voltage. The bonded areas of wafer pairs were measured under visible light. The impurity concentration in the bonded glass measured by SIMS was compared with that in a standard glass substrate. A hermetically sealed silicon wafer was fabricated as a result of using the SDAB method.

3. Results and Discussion

3.1 Surface roughness of glass and silicon wafers

The surface roughness of the wafer is one of the most important parameters in the bonding process. A rough surface may be the main reason for failure in the bonding process. The surface roughness of the wafers used in the experiment was measured by AFM, and the measured images are shown in Fig. 2. The AFM results are summarized in Table I, where "Bare" indicates the pure silicon wafer [Fig. 2(a)] and pure glass wafer [Fig. 2(b)]. Group B denotes the silicon wafer [Fig. 2(c)] and glass wafer [Fig. 2(d)] after RCA cleaning and hydrophilization. The glass wafer had a higher surface roughness than the silicon wafer. It was confirmed that the average surface roughness of group B samples increased nearly two times, compared to that of the bare glass and silicon.

3.2 Comparison of bonded area after bonding process

The nonbonded areas between the bonded glass-to-silicon wafer pairs were measured under the illumination of visual light. The typical features of the samples belonging to group A and group B are shown in Figs. 3(a) and 3(b), respectively. The samples of group B were initially bonded by hydrophilization without annealing, then anodic bonding was carried out under the same condition as for group A. These samples were bonded at a temperature of 250°C with dc voltage of 300 V. In the case of group A, the bonded area occupied more than 10% of the whole wafer area, but the nonbonded area is apparent in the side area, as shown in Fig. 3(a). In case of group B, on the other hand, the bonded area occupied more than 70% of the whole wafer area. In order to characterize the effect of the bonding voltage on the bonded area, the specimens of group A and group B were bonded at a temperature of 300°C with applied voltages of 250 V and 300 V, respectively. The obtained experimental results were presented in Fig. 4. The results in Figures 3 and 4 show that the bonded area increased with increasing applied voltage and temperature. This increase induced a large electrostatic force and resulted in allowed strong bonding. Also, in the samples of SDAB, initial bonding at room temperature takes place as a result of interaction between Si–OH groups formed due to hydrophilicity and pulls them together by Van der Walls force. Increased electrostatic force results because of the decreased gap between the glass and silicon wafer. Therefore, we suggest that the migration rate of the sodium ions in the glass wafer is higher than in the case of the anodic process only, which in turn result in a wider bonded area.

3.3 Current and time characteristics of bonding process

In order to characterize the bonding process, current-time characteristics were measured for group A and group B during the start period. The bonding current was measured at

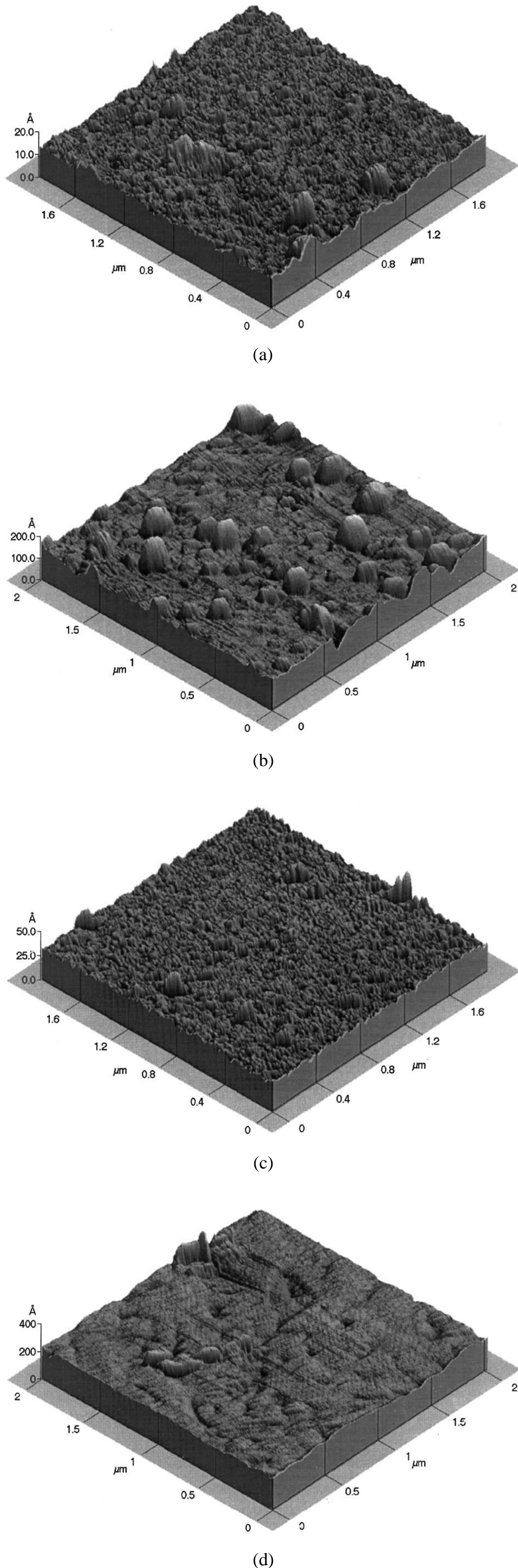

Fig. 2. AFM image of (a) bare silicon and glass, (b) silicon and glass of group B after hydrophilization.

Table I. Roughness parameters of AFM images for silicon wafer and glass wafer.

Parameter	Wafer			
	Silicon		Glass	
	Bare	Group B	Bare	Group B
Peak to valley (Å)	17	39	174	274
Median height(Å)	5.1	14	69	96
Ave. roughness(Å)	1.1	2.0	12	12

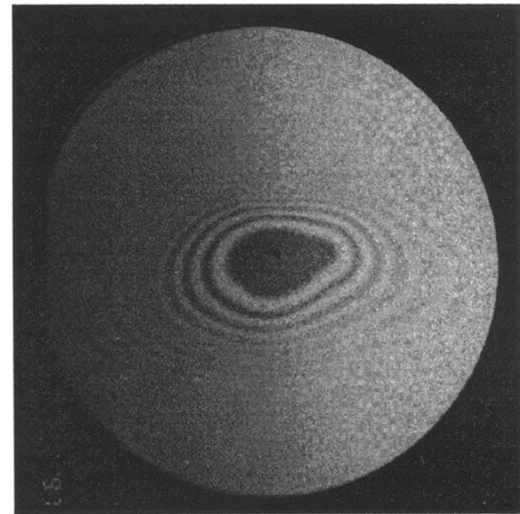

(a)

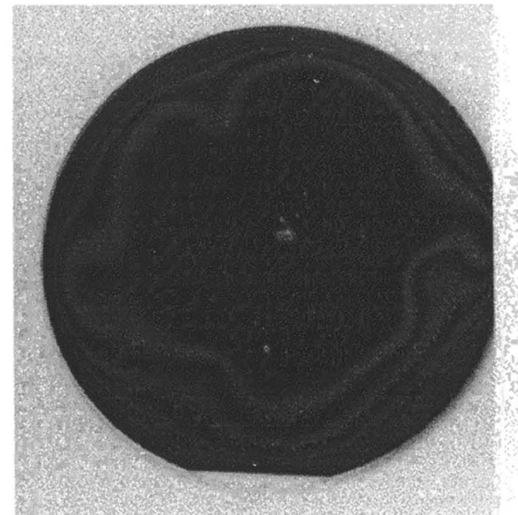

(b)

Fig. 3. Image of bonded area for (a) group A and (b) group B.

300°C with an applied voltage of 250 V for 10 min. The bonding current decayed rapidly and then remained at a minimum level, as shown in Fig. 5. The obtained current density profile was well fitted with a typical current-time relationship in the anodic bonding process. The bonding current is due to the transport of sodium ions in the glass wafer. Figure 5 shows that the bonding current of group B was higher than that of group A. We infer that initial bonding by the hydrophilic process reduced the gap between silicon and glass wafer, resulting in a higher diffusion rate of the sodium ions which in turn

(a)

(b)

Fig. 4. Comparison of the bonded area with changed dc voltage for (a) group A and (b) group B.

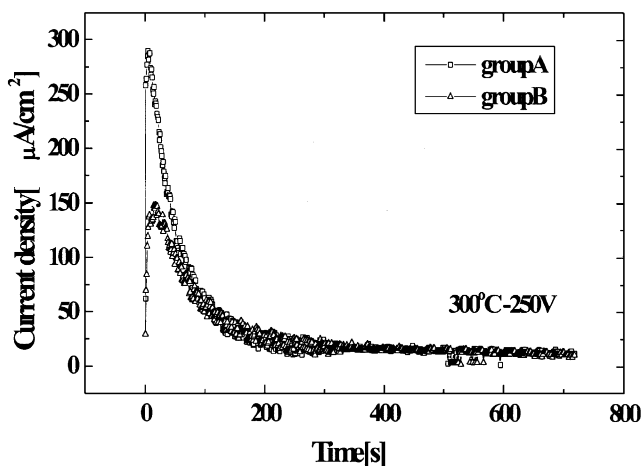

Fig. 5. Current-time characteristics.

causes a higher bonding current.

3.4 *Tensile strength of the bonded wafer pairs*

In order to determine the bond strength of the glass-to-silicon wafer pairs, the tensile strength method was employed. The obtained result is illustrated in Fig. 6. The bonding strength is plotted as a function of applied voltage at a temperature of 330°C [Fig. 6(a)] and as a function of temperature at the applied voltage of 350 V [Fig. 6(b)]. It is shown that group B has higher strength than group A under the same conditions. The strength of bonded wafers was obtained from measured strength divided by the bonded area. Upon increasing the bonding temperature from 200 to 300°C and the bonding voltage from 60 to 300 V, the bonding strength increases and reaches the bulk bonding strength of the Pyrex glass substrate (lower than 25 MPa). In all samples, breakage occurred in the glass or silicon-glass interface.[5,11] The limit of measurement is 20 MPa with our equipment. Destruction above 20 MPa infers the bulk bonding strength of glass. In our experiment, the bond strength obtained by a tensile strength method was between 0.1 MPa and 20 Mpa. Above 20 MPa, bonded bulk Pyrex #7740 glass was disrupted for all specimens.

In these results, the specimen bonded using SDAB (group B) had higher tensile strength than that bonded using anodic bonding (group A) only. In general, the strength of bulk glass has been reported to be lower than 25 MPa.[12]

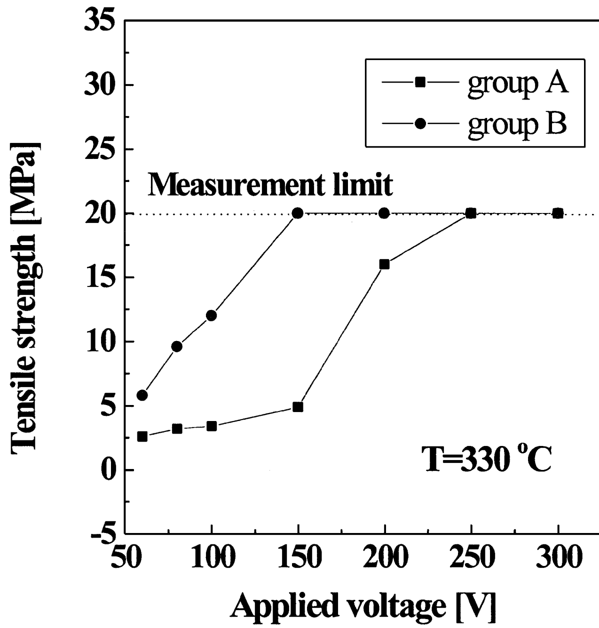

(a)

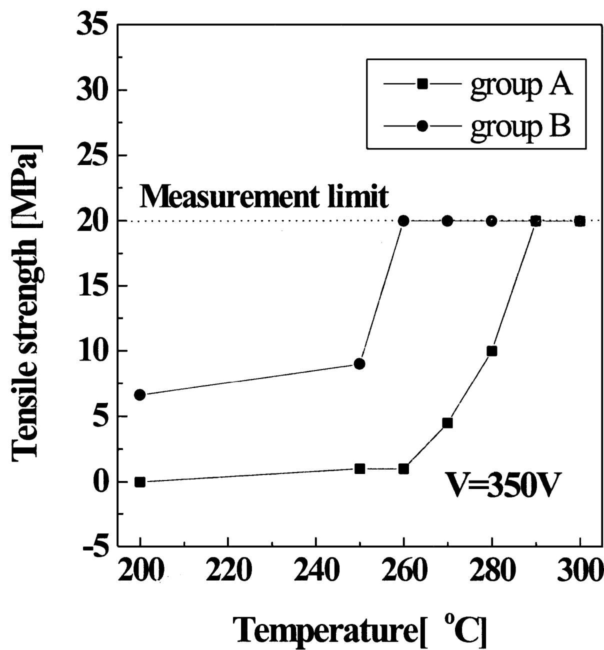

(b)

Fig. 6. Tensile strength characteristics for group A and group B as function of (a) the applied voltage and (b) the bonding temperature.

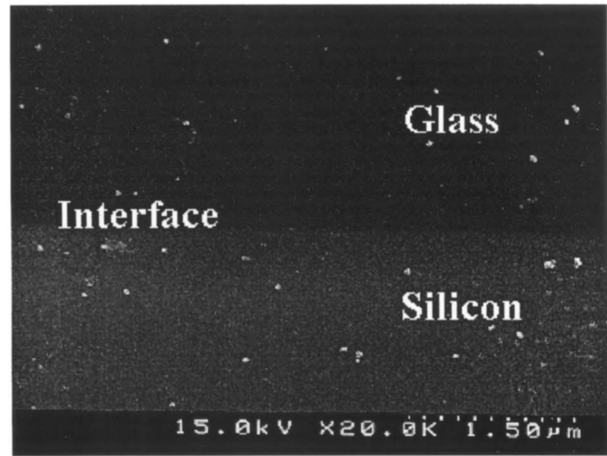

Fig. 7. SEM micrographs of the bonded interface region for group B.

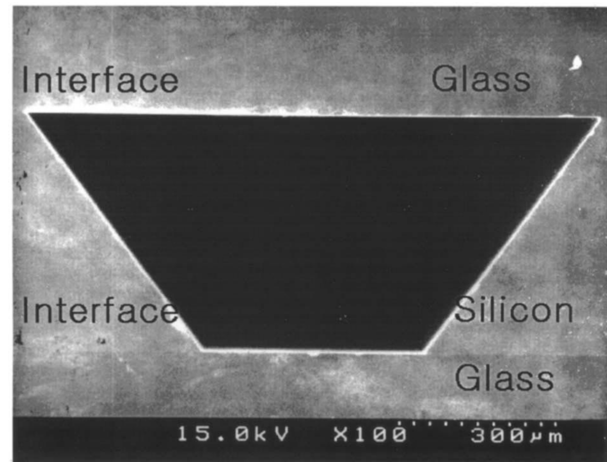

(a)

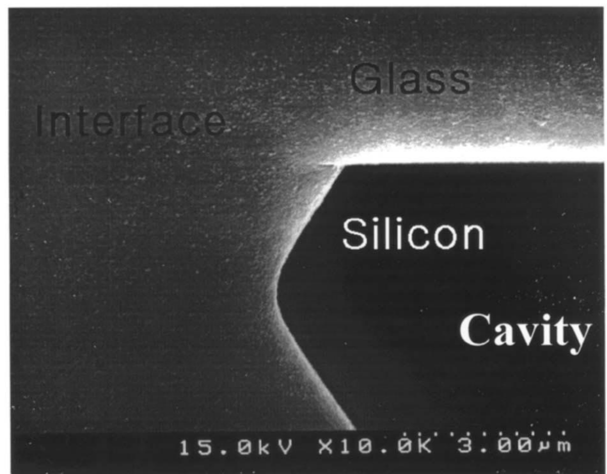

(b)

Fig. 8. SEM micrographs of the multiple bonded interface region. (a) Structure of multiple Bond. (b) Interface region between silicon and upper glass.

3.5 Comparison of the interface region using SEM

The specimens were cut and polished to investigate the cross-sectional bonded interface region of the glass-to-silicon assembly. The samples were bonded at the dc voltage of 350 V and temperature of 300°C. Figure 7 shows the scanning electron microscopy (SEM) micrograph of the interface region of group B. The white spots are grains of alumina powder used in polishing.

3.6 Cross-sectional SEM view of hermetically sealed silicon wafer

Figure 8(a) shows a SEM micrograph of the cross-sectional view of the hermetically sealed silicon wafer by the SDAB method. The structure can be applied for the sealing of micromachined sensors. A cavity of 1 mm × 2 mm × 500 μm was formed on the silicon substrate by anisotropic etching of

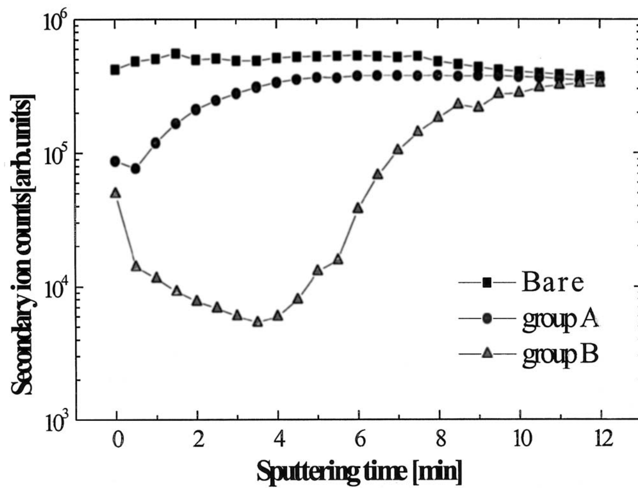

Fig. 9. Relative depth profiles of Na for the surface region of glass wafers after debonding.

the silicon substrate in ethylenediamine-pyrocatechol-water (EPW). We performed bonding with multiple layers in a glass-silicon-glass sandwich structure. Negative voltage was applied to the upper and the lower glass simultaneously. Finally, the cavity was sealed by multiple bonding of the two glass wafers. Figure 8(b) shows a SEM micrograph of the interface region between silicon and the upper glass wafer.

3.7 Role of the sodium ion in the bonding process

Sodium ion plays a very important role in anodic bonding. A region depleted of sodium ions results in electrostatic force that pulls them together, leading to the formation of atomic bonds. In order to investigate the migration of sodium ions during the bonding process, SIMS analysis was carried out on the surface of glass wafers. The bonding temperature was 300°C and applied voltage was 250 V. The wafer pairs were debonded by inserting a blade into the bonded interface. The SIMS data obtained from the surface of a bare Pyrex #7740 glass wafer with the sputtering rate of 100 Å/min were compared with those for the surfaces of group A (anodic) and group B (SDAB) glass wafers. Figure 9 shows the relative depth profile of a glass wafer before and after bonding. It is apparent that the sodium ions were depleted in the surface region of the glass wafer in contact with the silicon wafer to be bonded. In the case of SDAB, we can clearly observe that the depletion region of sodium ions is deeper than that in group A samples. It is well known that a deeper depletion region results in having a stronger bonding strength. Therefore, we propose that the deeper depletion region in the case of SDAB results in a higher efficiency than when using the anodic bonding process.

4. Conclusion

In order to modify silicon-to-glass wafer anodic bonding in a conventional environment, we employed the SDAB process of initial bonding of a hydrophilized wafer. The improved bonding properties using SDAB were discussed based on the measured strength, current-time curve and the SIMS analysis before and after bonding. A wide bonded area, higher tensile strength, increased bonding current and deeper depletion layer were obtained. As mentioned above, the SDAB method shows superior characteristics than other methods. It is believed that the decrease of the gap between glass and silicon wafers in the initial hydrophilic bonding process produces higher electrostatic force, based on the result of the current-time curve and depth profile. As a result, it is possible to enhance the bonding efficiency by adopting the SDAB process. The results indicate that the process can be applied to vacuum packaging of microelectronic devices and microsensors.

Acknowledgments

This work was supported by the Ministry of Science and Technology and the Ministry of Industry and Energy of Korea. The authors wish to thank J. H. Jung and H. W. Park of KIST for assistance in this work.

1) C. D. Fung, P. W. Cheung, W. H. Ko and D. G. Fleming: *Micromachining and Micropackaging of Transducer* (Elsevier Science, Amsterdam, 1985) p. 41.
2) B. K. Ju: Dr. Thesis, Korea University, Seoul, 1995 p. 8.
3) B. Puers, E. Peeters, V. D. Bossche and W. Sansen: Sens. & Actuat. **A 21–23** (1990) 8.
4) B. Puers and D. Lapadatu: Sens. & Actuat. **A 41–42** (1994) 129.
5) G. Wallis and D. I. Pomerantz: J. Appl. Phys. **40** (1969) 3946.
6) K. Gustafsson, B. Hok, S. Johansson and T. Muttay: Sens. & Mater. **2** (1988) 65.
7) A. D. Kurtz, J. R. Mallon and H. Bernstein: ISA ASI 73246 (1973) 229.
8) M. Esashi and A. Nakano: Sens. & Actuat. **A21–23** (1990) 931.
9) M. Shimbo, K. Furukawa, K. Fukuda and K. Tanzawa: J. Appl. Phys. **60** (1986) 2987.
10) R. Stengl, T. Tan and U. Gosele: Jpn. J. Appl. Phys. **28** (1989) 1735.
11) E. Obermeier: Electrochem. Soc. Proc. (1995) 95-7, p. 212.
12) A. Cozma and B. Puers: Micromechanics Europe 1994 Workshop Dig., 1994, p. 40.